Vertical Distribution of Temperature and Contaminant Concentration in a Room with Impinging Jet Ventilation System

Mako Matsuzaki*[1], Tomohiro Kobayashi[1], Toshio Yamanaka[1], Narae Choi[1], Haruna Yamasawa[1]

1 Osaka University
Suita 565-0871
Osaka, Japan
**matsuzaki_mako@arch.eng.osaka-u.ac.jp*

ABSTRACT

The impinging jet ventilation system (hereinafter referred to as IJV) has been proposed as a new air conditioning ventilation system. Properties of indoor environment with this system using impinging jet are complicated. The present paper reports fundamental properties of indoor air with distributed interior heat generation load assuming an office.
The experiment was conducted in the climate chamber of which floor area was 27.0 m^2, and basic properties of temperature and CO_2 distributions were investigated. Heat load within a room was simulated by black lamps (incandescent bulb covered with dark purple glass) distributed uniformly. As for contaminant, CO_2 was generated from 4 locations. The temperature and CO_2 concentration were measured by changing the combination of supply air temperature and supply air flow rate, and four cases were studied. In addition, the number of IJV supply terminals was also changed as a parameter to understand the effect of supply air momentum. Two cases (1 or 2 terminals) were studied without changing total supply airflow rate, i.e., only supply momentum was changed. In total eight cases were studied in the experiment. The specific Archimedes number was defined and evaluated based on experimental results, and relationship between temperature/concentration stratification and Archimedes number was investigated. It was shown that the temperature/concentration stratification become clear when the supply airflow momentum is small. Moreover, a correlation between Archimedes number and vertical temperature difference was shown. To propose a simplified calculation model, further parametric study is required, and CFD analysis seems to be beneficial because it enables numerical experiment easily. To do this, however, CFD calculation method for IJV system needs to be validated. Therefore, one case of full-scale experiment was simulated. Here, the effect of turbulence model was evaluated, and three turbulence models (standard k-ε model, RNG k-ε model, and SST k-ω model) were studied, and the accuracy of CFD analysis is finally verified.

KEYWORDS

Impinging Jet, Temperature Stratification, Full-scale Experiment, Quasi Displacement Ventilation, Thermal Stratification, CFD analysis

1 INTRODUCTION

As an air distributing system with high ventilation efficiency, a displacement ventilation system is well known. However, this supply system can only be used for cooling mode, and may generate excessive vertical temperature difference. To overcome these disadvantages, the IJV system *[1]* has been proposed. IJV system is an air distributing strategy that supplies air horizontally from the bottom of the room by using impinging jet. The impinging jet is generated by blowing the jet downward from ducts installed on the wall and impinging on the floor surface. To date, however, few studies have been done on the indoor environment created by IJV system. In previous studies *[2] [3]*, in order to understand the fundamental tendency of the

thermal environment created by IJV system in a large space with high heat load such as a factory, where IJV system seems to be beneficial, the laboratory experiment, CFD analysis and model calculation were conducted for a room model with high heat generation load at the center of the room. In order to investigate the performance of the IJV system for more general environment like an office, a full-scale experiment and CFD analysis were conducted for a room with uniformly distributed heat load. The final purpose of this study is to propose a simplified calculation method of vertical distribution of temperature and contaminant concentration that can be used in the design phase. This paper first presents the results of the full-scale experiment. Then, the CFD analysis which simulates the experiment is conducted to verify its accuracy.

2 FULL SCALE COOLING EXPERIMENT

2.1 Experimental Room

The experiments were conducted from January 29th, 2019 to February 14th, 2019 at a full-scale climate chamber (5,450(d)×5,000(w) ×2,770(h)[mm]) in Osaka University, Japan. The floor plan and cross-section of the chamber are shown in Figure 1 and 2, respectively. Two round ducts whose diameter were 150 mm were provided as IJV supply terminals, and the height of their bottom end was set at 600 mm above the floor level. These IJV supply ducts were insulated by foamed polyethylene sheets. The supply air flow rate was adjusted using a volume damper and an orifice flow meter (Iris Damper, Continental Fan). The room air was sucked out from an exhaust opening located on the ceiling. To simulate four occupants and all other interior heat generation in an office, 20 black lamps (50W × 20) were distributed in the chamber. The details of the assumed indoor heat load are shown in Table 1.

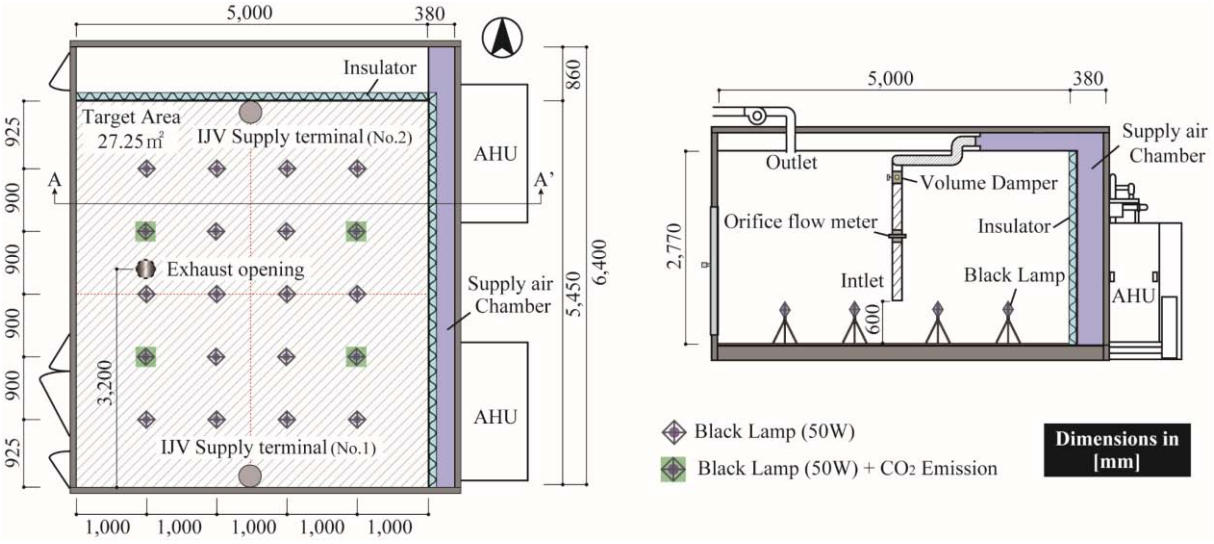

Figure 1: Floor plan and A-A' Cross-Section of the climate chamber

Table 1: Details of heat load

Sensible heat load of occupants (60[W/person])	Other heat load (28[W/m^2])	Total heat load [W]	Total heat load per unit area [W/m^2]
240	760	1000	36.7

2.2 Experimental Conditions

In the chamber, steady-state non-isothermal experiments were conducted to understand the effect of the correlation between supply airflow momentum and buoyancy (temperature difference from supply to ambient air) on the temperature and CO_2 concentration distribution. To investigate this under the same condition of input heat rate, both supply air temperature and supply airflow rate were varied. The experimental conditions are shown Table 2. Here, supply air temperature was set by assuming perfectly insulated enclosure and 17 °C of the exhaust temperature for all cases. Additionally, the number of IJV inlet terminals was changed, which enables the comparison of different supply momentum conditions under the same total supply airflow rate. Since the experiments were conducted in winter, the outside temperature of the climate chamber (the chamber is a large space laboratory not air conditioned) was 7-12 °C. Generally, the setting point temperature for cooling is approximately 26 °C. However, it might cause excessive continental fan heat loss through the wall of the climate chamber because of large temperature difference if this temperature was assumed as the experimental condition of exhaust temperature. Therefore, to decrease the heat loss through the walls, assumed exhaust temperature was set at 17 °C.

Table 2: Experimental conditions

No	Number of IJV terminal	Assumed Exhaust Temperature [°C]	Heat Load [W]	Supply Temperature [°C]	Total Supply flow rate [m^3/h]				Supply velocity [m/s]
					250	300	375	500	
1	2	17	1000	5	X				1.96
2	2	17	1000	7		X			2.36
3	2	17	1000	9			X		2.95
4	2	17	1000	11				X	3.93
5	1	17	1000	5	X				3.93
6	1	17	1000	7		X			4.72
7	1	17	1000	9			X		5.89
8	1	17	1000	11				X	7.86

2.3 Measurement item

In the experiments, the distribution of temperature and CO_2 concentration were measured. The measurement points are shown in Figure 3. Temperature measurement was conducted by T-type thermocouple. The vertical temperature profile was obtained at 7 poles, where 24 measurement points were provided vertically for each, including the surface temperature of ceiling and floor. The measurement points on the north-south line is shifted by 200 mm from the center, so as not to barrier the development of the jet along the floor. The wall surface temperature was measured at 24 points for each wall. The CO_2 concentration was measured using 9 portable CO_2 concentration recorders provided vertically for each pole. CO_2 concentration was also recorded at the supply air chamber, the exhaust duct, and outside the climate chamber. After the temperature got to the steady state, CO_2 gas started to be emitted continuously with 15 L/h at each of the four emission points shown in Figure 1. Flow rate of CO_2 was regulated by the pressure reducing valve, and was emitted by inserting the tube into the sponge placed above the black lamp to decrease the initial velocity. The steady state result of both the temperature and CO_2 concentration was averaged for 30 minutes. (measurement interval:1 min)

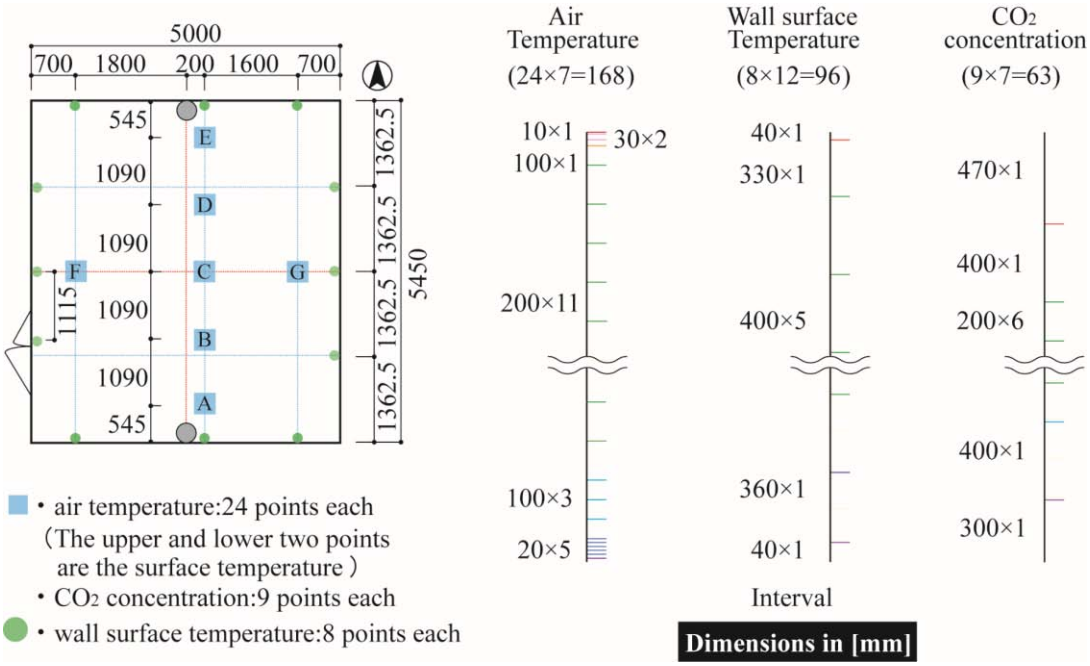

Figure 2: Measurement point of Temperature and CO_2 concentration

2.4 Experimental result

2.4.1 Temperature distribution

Temperature contours of the north-south central cross-section and vertical distribution of horizontal-averaged room temperature are shown in Figure 4 and 5, respectively. Under the condition of small supply air flow rate, indoor air temperature was vertically stratified. As the supply air flow rate increases, indoor air temperature distributed uniformly. Regarding the number of IJV terminal, the temperature distribution in the room was more uniform at single IJV terminal conditions, whose supply air momentum was relatively high, than two IJV terminal conditions. Supply temperature, exhaust temperature, external temperature, heat loss due to heat transmission through the wall calculated from the heat balance, heat load measured using a watt meter and heat loss ratio (ratio of heat loss and heat load) are summarized in Table 3. The temperature difference of the exhaust air for each condition seems to be caused by the effect of the external temperature. In most cases, the heat loss tended to increase as the external temperature decreased, and the maximum heat loss ratio was 18 %, which cannot be regarded as negligible. Although the insulation needs to be improved for further detailed study, we interpreted that the experiment was helpful for understanding the fundamental physics.

Table 3: Supply/Exhaust/External Temperature, and Heat loss

No	Number of IJV terminal	Supply Temperature [°C]	Exhaust Temperature [°C]	External Temperature [°C]	Heat Load [W]	Heat loss [W]	Heat loss ratio [%]
1	2	4.61	16.08	9.56	993	38	4
2	2	6.70	16.32	10.59	997	34	3
3	2	8.67	15.60	9.42	1001	135	13
4	2	10.83	16.31	11.81	995	81	8
5	1	4.61	14.43	6.78	991	173	17
6	1	6.58	15.21	9.18	979	116	12
7	1	8.45	15.13	7.93	1005	170	17
8	1	10.77	15.67	9.66	990	177	18

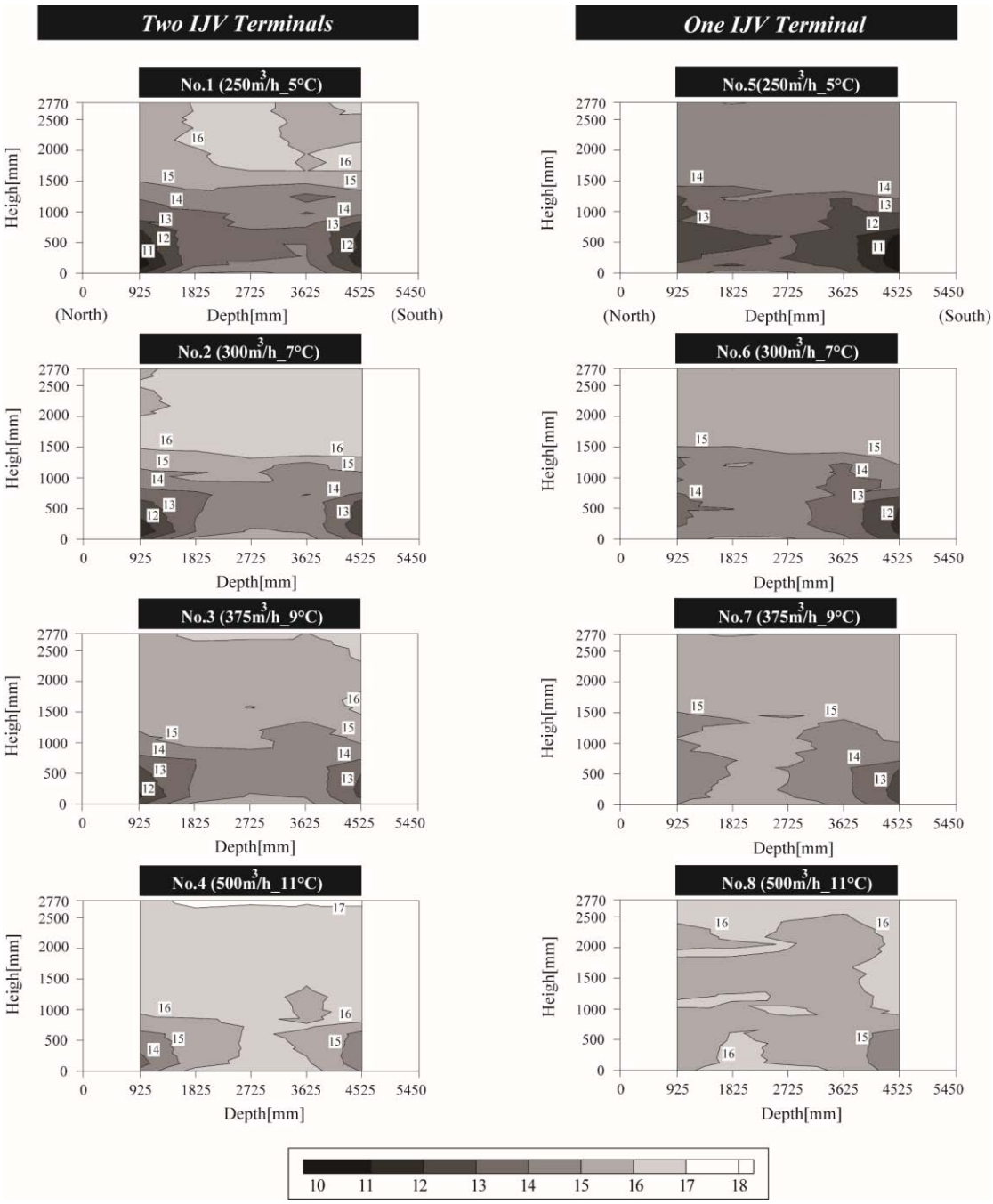

Figure 3: Temperature Contour

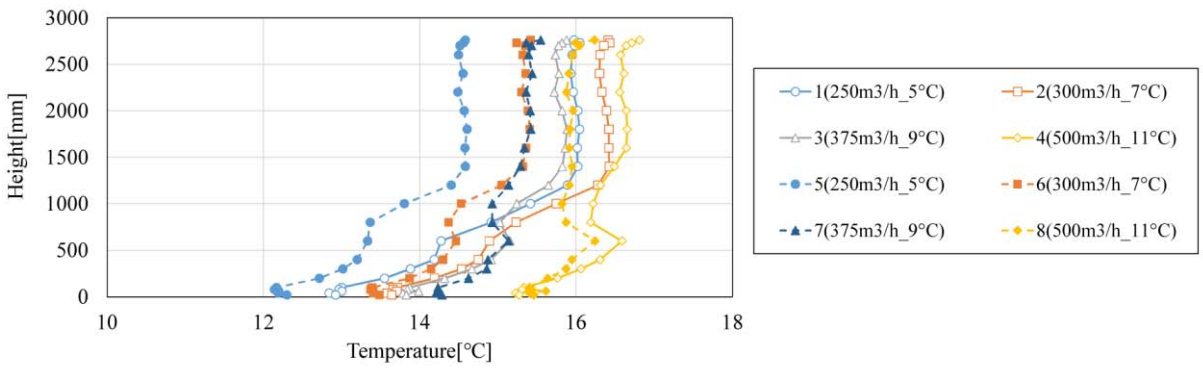

Figure 4: Vertical distribution of horizontal-averaged room Temperature

2.4.2 Normalized CO_2 concentration distribution

The normalized CO_2 concentration contours on the north-south central cross-section and vertical distribution of horizontal-averaged room normalized CO_2 concentration are shown in Figure 5 and 6, respectively. For normalization, CO_2 concentration at each measurement points were subtracted by that of supply air, and divided by the concentration difference between exhaust and supply air. As shown in Figure 5, CO_2 concentration generally stratified vertically. As the supply air flow rate decreases, the CO_2 concentration stratification inside the room got more clear. In addition, it was found that the stratification of CO_2 concentration is clearer than that of temperature because CO_2 works like passive contaminant.

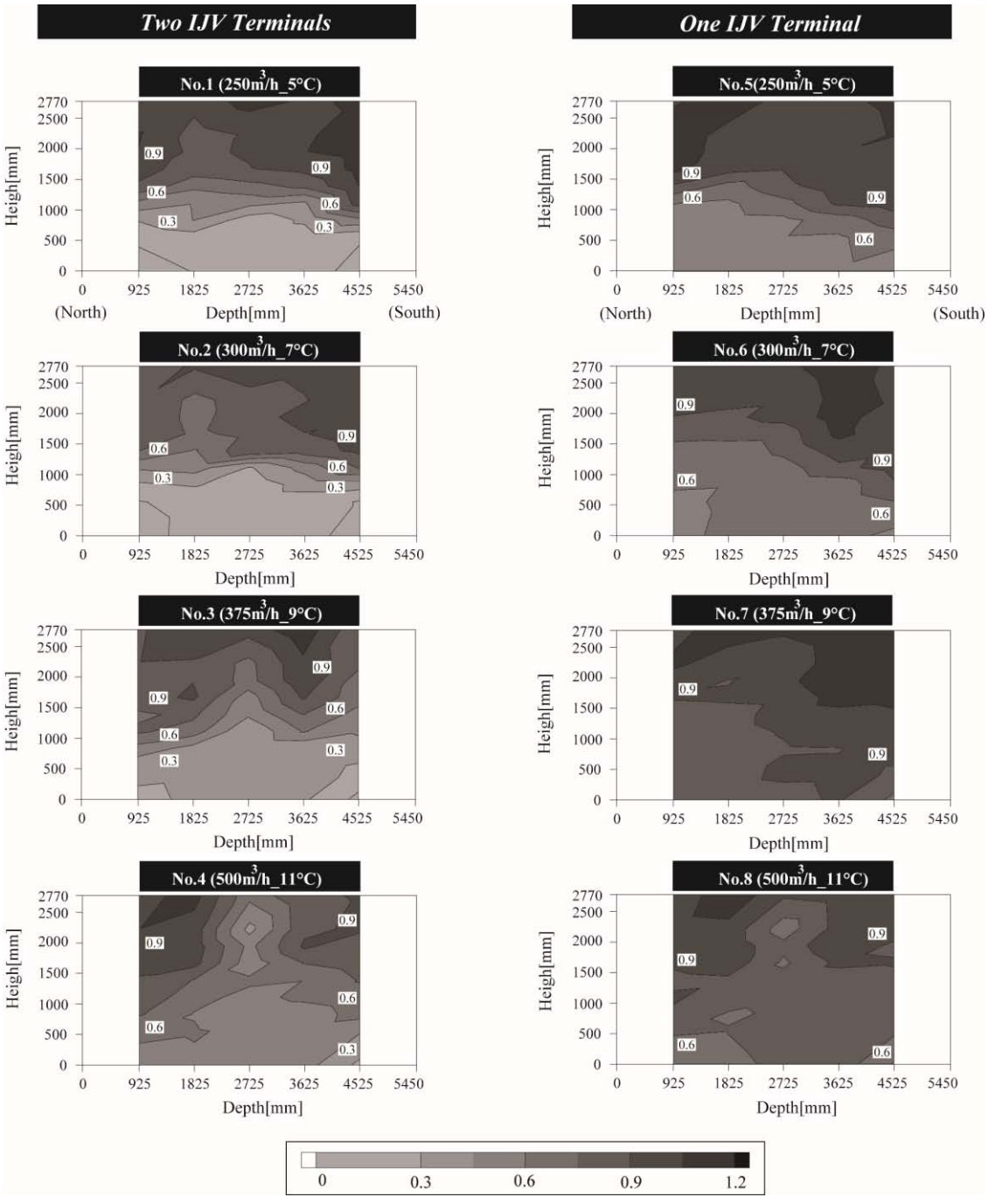

Figure 5: Normalized CO_2 concentration Contour

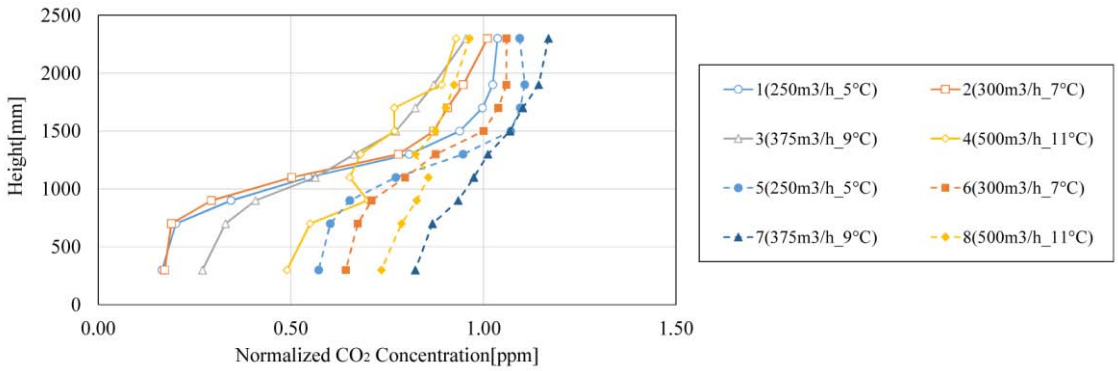

Figure 6: Vertical distribution of horizontal-averaged room Normalized CO_2 concentration

2.5 Archimedes number

It is considered that the ratio of buoyancy and supply airflow momentum has more or less influence on the formation of thermal stratification. Thus, the "Inlet Archimedes number" around the IJV supply terminal was defined in this paper:

$$A_{r(in)} = \frac{g\beta(T_\ell - T_s)D}{U^2} \tag{1}$$

where T_ℓ [°C] is the average temperature in the lower part of the chamber (20 to 100 mm above the floor), T_s [°C] is supply air temperature, T_e [°C] is exhaust air temperature, D [m] (=0.15) is the diameter of the terminal, g [m/s^2] (=9.81) is acceleration of gravity, U [m/s] is supply air velocity, and β [1/K] is volume expansion coefficient. The variables and Archimedes numbers are shown in Table 4, and the correlation between Archimedes number and dimensionless temperature difference is shown in Figure 6. The dimensionless temperature difference was defined as:

$$\Delta T^* = \frac{T_e - T_\ell}{T_e - T_s} \tag{2}$$

where, ΔT^* is a measure of temperature distribution, i.e. ΔT^* approaches to 1 when the temperature stratification was formed, and ΔT^* approaches to 0 when the temperature distribution was uniform. In Figure 6, it is shown that ΔT^* approaches to the constant value which depends on the chamber insulation and the outside temperature of the chamber, as $A_{r(in)}$ increases, thus it was confirmed that $A_{r(in)}$ has correlation with ΔT^*. Therefore, air temperature distribution varies by changing the number of supply inlet and supply air condition, even if the heat load is the same.

Table 4: Value of variable and Archimedes number

No	U[m/s]	T_e[°C]	T_s[°C]	T_ℓ[°C]	β[1/K]	Ar×10^{-3}[-]	Δ T*[-]
1	1.96	16.08	4.61	12.95	0.00360	11.43	0.27
2	2.36	16.32	6.70	13.66	0.00357	6.59	0.28
3	2.95	15.60	8.67	13.86	0.00355	3.12	0.25
4	3.93	16.31	10.83	15.31	0.00352	1.50	0.18
5	3.93	14.43	4.61	12.20	0.00360	2.60	0.23
6	4.72	15.21	6.58	13.41	0.00357	1.62	0.21
7	5.89	15.13	8.45	14.24	0.00355	0.87	0.13
8	7.86	15.65	10.77	15.46	0.00352	0.39	0.04

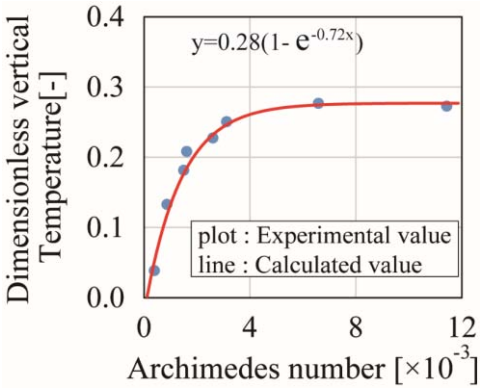

Figure 7: Correlation between Inlet Archimedes number and dimensionless vertical temperature difference

3 ACCURACY VERIFICATION OF CFD ANALYSIS

3.1 Computational domain

It seems beneficial to use CFD because it facilitates the parametric study regarding several important parameters. As the preliminary step, the accuracy of CFD analysis needs to be verified by comparing the results with experiment. The computational domain was assumed to be indoor space of the chamber in the previous chapter, and a full-scale model was constructed as shown in Figure 7.

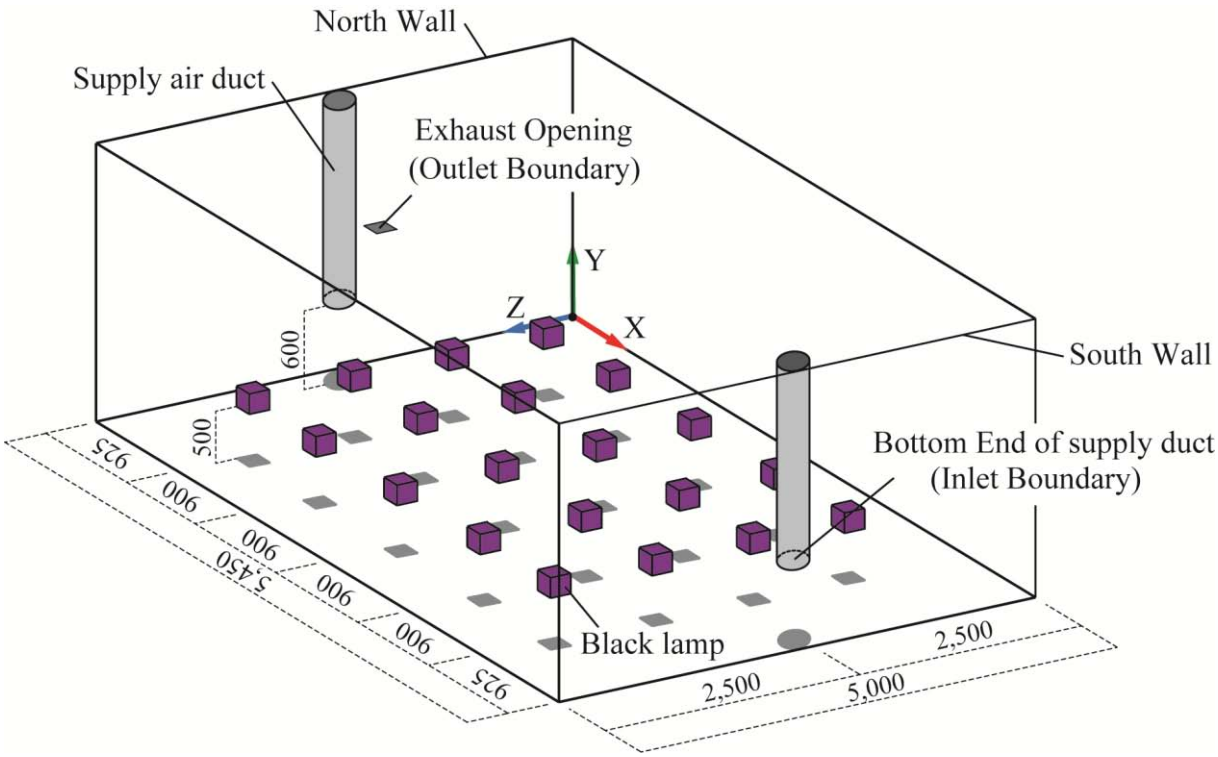

Figure 8: Computational domain

The analysis was conducted under the experimental condition 1 in Table 3. The distributed indoor heat loads were 1,000 W in total, and two IJV terminals were placed at the center of walls, one at the north wall and the other at the south wall. The inlet boundary was set at the bottom end of the supply duct (600 mm above the floor) with the supply air flow rate of 250 m^3/h, which corresponds to 1.96m/s of the inlet velocity, and the supply air temperature was set at 4.61 °C. The analysis was conducted in a non-isothermal condition, and the buoyancy was expressed by Boussinesq approximation. The heat load was simulating by considering spatial energy source term (=50,000[W/m^2]). The thickness, heat conductivity and external temperature were given as the thermal boundary condition at the wall and ceiling. Since the floor was located on the ground, the boundary condition was set as insulation. The radiation was also solved based on surface to surface radiative heat transfer model, and the analysis was steady state. Total number of cells was 3,250,474. Three types of turbulence model, which were SST k-ω, Standard k-ε and RNG k-ε, were compared. The summary of the CFD calculation setting is summarized in Table 5.

3.2 Examination of turbulence model dependency

The temperature profiles along five vertical lines in north-south central line (z=2,500[mm]), which correspond to the poles in the experiment, obtained from different turbulence models were compared with experimental result in Figure 8. As shown in Figure 8, analysis results agreed relatively well with experimental result at the upper part of the room, while there were large errors at the lower part. It may be due to the adiabatic boundary condition at the floor. Since the supply air temperature is very low in the experiment, the heat came into the room through the floor when the supply air was impinging on the floor. However, the boundary condition of the floor was set as adiabatic, thus the analysis results underestimated the heat transmission through the floor, which resulted in difference in the lower part. Regarding the turbulence model, the standard deviation of the temperature difference between experimental and analysis was the smallest in the case of SST k-ω model. It was shown that the boundary condition at the floor needs to be reconsidered for improving the accuracy of CFD.

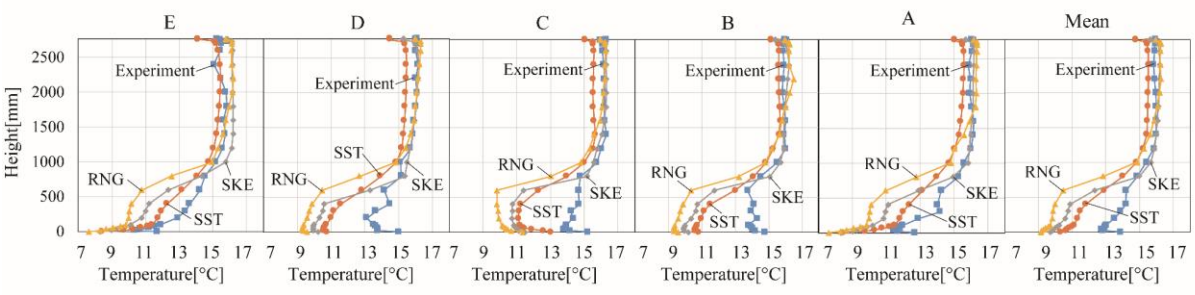

	Turbulence model	Standard Deviation
No1	SST k-ω(SST)	1.688
No2	Standard k-ε(SKE)	2.047
No3	RNG k-ε(RNG)	2.556

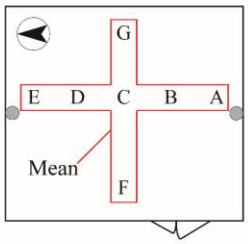

Figure 9: Experimental values and calculated values with different turbulence model and standard deviation

Table 5: Summary of the CFD Calculation Setting

Studied Case			**No.1**	**No.2**	**No.3**
CFD code			Ansys Fluent 19.2		
Turbulence Model			SST k-ω	Standard k-ε	RNG k-ε
Radiation Model			Surface-to-Surface Model		
Algorithm			SIMPLE		
Discretization scheme for Advection Term			QUICK	Second order upwind	QUICK
Boundary Condition	**Inlet**		Velocity Magnitude U=1.96[m/s]		
			Turbulent Intensity I=10[%]		
			Turbulent Length Scale L=10.5[mm]		
			Temperature T=4.61[°C]		
	Outlet		Velocity Magnitude U=-6.94[m/s]		
	Walls	**Velocity**	Linear-Logarithmic Blending Law	Standard Wall Function	
		Floor	Adiabatic Boundary (0[W/m^2])		
		Other walls	External Temperature		
Cell Zone Condition	**Black Lamp**		Energy source 50,000[W/m^3]		
Total Number of cells			3,250,474		

4 CONCLUSIONS

In order to understand the environment formed by IJV system in a room with uniformly distributed heat generation load, both the experiment and CFD analysis were conducted. The supply air conditions were changed as a parameter in this paper. The findings obtained in this paper are summarized follows:

- In the experiments, under the condition of small supply air flow rate, indoor air temperature distribution was vertically stratified, while under the condition of large supply air flow rate, indoor air temperature distributed uniformly.
- The distribution of CO_2 concentration stratified clearer than that of temperature.
- Air temperature distribution varies by changing the number of supply inlet and supply air condition, even if the heat generation load is the same.
- In CFD analysis, results agreed relatively well with experimental result at the upper part of the room, while there were large errors at the lower part. This may be due to the adiabatic boundary condition at floor. Consequently, it seems necessary to change the boundary conditions considering heat loss to improve the accuracy.

5 REFERENCES

[1] T.Karimipanaha, H.B.Awbi (2002) Theoretical and experimental investigation of impinging jet ventilation and comparison with wall displacement ventilation. Building and Environment, Vol.37, pp.1329‑1342.

[2] Tomohoro KOBAYASHI, Kazuki SUGITA, Noriko UMEMIYA (2016) A Study on Semi-Displacement Ventilation using Impinging Jet Flow. Journal of Environmental Engineering (Transactions of AIJ), Vol.81, No.730, pp.1117‑1125. (In Japanese)

[3] Atsushi TOMITA (2014) Fundamental Study onTemperature and Airflow Distribution in Semi-Displacement Ventilation using Radial Wall Jet, Part 3. Proceedings of Annual Meeting of SHASE Kinki Chapter, pp.413‑416. (In Japanese)